REPORT DOCUMENTATION PAGE

Form Approved
OMB No. 0704-0188

1. AGENCY USE ONLY (Leave blank)	2. REPORT DATE	3. REPORT TYPE AND DATES COVERED
	April 1, 1996	Reprint

4. TITLE AND SUBTITLE
Production of vibrationally and rotationally excited NO in the nighttime terrestrial thermosphere

5. FUNDING NUMBERS
PR 2303
TA GD
WU 06

6. AUTHOR(S)
R. D. Sharma
Hoang Dothe*
F. von Esse*
V.A. Kharchenko**
Y. Sun**
A. Dalgarno**

7. PERFORMING ORGANIZATION NAME(S) AND ADDRESS(ES)
Phillips Laboratory/GPOS
29 Randolph Road
Hanscom AFB, MA 01731-3010

8. PERFORMING ORGANIZATION REPORT NUMBER
PL-TR-96-2071

9. SPONSORING/MONITORING AGENCY NAME(S) AND ADDRESS(ES)

11. SUPPLEMENTARY NOTES Reprinted from Preprint Series, Harvard College Obs; Smithsonian Astrophysical Observatory, 60 Garden Street, Cambridge, MA 02138
* Mei Technology Corporation, 1050 Waltham street, Lexington, MA 02173
** Harvard-Smithsonian Cntr for Astrophysics, 60 Garden Street, Cambridge, MA 02138

12a. DISTRIBUTION/AVAILABILITY STATEMENT
Approved for public release; distribution unlimited

12b. DISTRIBUTION CODE

13. ABSTRACT (Maximum 200 words)

A quantitative interpretation is given of the observed quiescent nighttime radiance of nitric oxide in the fundamental vibration-rotation band near 5.3 um. The radiance measured in the space shuttle experiment CIRRIS-1A is known to have two components, one characterized by a thermal population of rotational levels and the other by a highly excited rotational population. The analysis presented here confirms that the thermal population is due to impact excitation of NO by atomic oxygen and attributes the highly excited distribution to the reaction of N(4S) atoms with O2. The measured nighttime emission profile is compared with predictions for several model atmospheres. Both sources of excited NO depend upon latitude, longitude, local time, and geomagnetic indices. The fraction of vibrationally excited NO produced by the reaction of N(4S) with O2 increases rapidly with altitude from 130 to 200 km and its contribution to cooling, though less than that from inelastic excitation of NO(v=0) is, at higher altitudes, comparable to cooling produced by the atomic oxygen fine-structure line at 63 um.

14. SUBJECT TERMS	15. NUMBER OF PAGES
infrared emission, vibration-rotation bands, cooling rates, rotationally thermal emission, rotationally hot emission, inelastic scattering, reactive scattering	25
	16. PRICE CODE

17. SECURITY CLASSIFICATION OF REPORT	18. SECURITY CLASSIFICATION OF THIS PAGE	19. SECURITY CLASSIFICATION OF ABSTRACT	20. LIMITATION OF ABSTRACT
UNCLASSIFIED	UNCLASSIFIED	UNCLASSIFIED	SAR

Center for Astrophysics
Preprint Series No. 4286

PRODUCTION OF VIBRATIONALLY AND ROTATIONALLY EXCITED NO IN THE NIGHTTIME TERRESTRIAL THERMOSPHERE

R.D. Sharma
Optical Environment Division (GPOS), Geophysics Directorate, Phillips Laboratory

Hoang Dothe and F. von Esse
Mei Technology Company

and

V.A. Kharchenko, Y. Sun, and A. Dalgarno
Harvard-Smithsonian Center for Astrophysics

PRODUCTION OF VIBRATIONALLY AND ROTATIONALLY EXCITED NO IN THE NIGHTTIME TERRESTRIAL THERMOSPHERE

R. D. Sharma, Optical Environment Division (GPOS), Geophysics Directorate, Phillips Laboratory, 29 Randolph Road, Hanscom AFB, MA 01731-3010

Hoang Dothe, F. von Esse, Mei Technology Co., 1050 Waltham Street, Lexington, MA 02173

V. A. Kharchenko, Y. Sun, and A. Dalgarno, Harvard-Smithsonian Center for Astrophysics, 60 Garden Street, Cambridge, MA 02138

ABSTRACT

A quantitative interpretation is given of the observed quiescent nighttime radiance of nitric oxide in the fundamental vibration-rotation band near 5.3 μm. The radiance measured in the space shuttle experiment CIRRIS-1A is known to have two components, one characterized by a thermal population of rotational levels and the other by a highly excited rotational population. The analysis presented here confirms that the thermal population is due to impact excitation of NO by atomic oxygen and attributes the highly excited distribution to the reaction of $N(^4S)$ atoms with O_2. The measured nighttime emission profile is compared with predictions for several model atmospheres. Both sources of excited NO depend upon the latitude, longitude, local time and geomagnetic indices. The fraction of vibrationally excited NO produced by the reaction of $N(^4S)$ with O_2 increases rapidly with altitude from 130 to 200 km and its contribution to cooling, though much less than that from inelastic excitation of NO(v=0) is, at higher altitudes, comparable to cooling by produced by the atomic oxygen fine-structure line at 63 μm.

I. INTRODUCTION

Cryogenic Infrared Radiance for Shuttle (CIRRIS-1A) was launched on 28 April 1991 aboard the space shuttle Discovery into a 260 km circular orbit at 57° inclination (Ahmadjian et al. 1990). Among the experiments conducted was the measurement of the infrared emission ($2.5 \leq \lambda \leq 25$ μm) from the terrestrial atmosphere with filtered radiometers and a high resolution (~1 cm^{-1}) Michelson interferometer. The spectra obtained in the 5.3 μm region, due to the fundamental vibration-rotation transitions of NO, were interpreted as a superposition of two components (Smith and Ahmadjian 1993, Armstrong et al. 1994). One component was attributed to a thermal population of rotational levels and the other to highly excited rotational levels. Both components are present during the day and night. There was some indication that the relative strength of the emission from the highly rotationally excited levels compared to that from the thermal component was less at night than during the day (Armstrong et al. 1994). A strong thermal component is expected from excitation of NO by collisions with oxygen atoms (Kockarts 1980, Zachor et al. 1985, Ballard et al. 1993)

$$NO(v = 0) + O \rightarrow NO(v = 1) + O. \qquad (1)$$

The rotational distribution in the v=1 level is expected to differ little from the distribution in the v=0 level (Quack and Troe 1979, Sharma et al. 1996). The daytime highly excited rotational component has been attributed to excitation in reactive collisions of energetic $N(^4S)$ atoms with O_2

$$N(^4S) + O_2 \rightarrow NO(v,J) + O \qquad (2)$$

(Sharma, Sun, and Dalgarno 1993). Armstrong et al. (1994) have suggested that reactions of energetic N atoms in the tail of the thermal Maxwell-Boltzmann distribution may be the source of the nocturnal emission. We carry out here quantitative calculations of the emission intensities of the two components for a range of nighttime conditions and compare the results with CIRRIS-1A measurements.

II. THE THERMAL COMPONENT

We use CIRRIS-1A data collected on day 119, year 1991, for which the tangent point altitudes span latitudes from -43.4° to -50.8°, longitudes from 30.5° E to 44.8° E and local times between 18.9 and 19.9 hrs., $F_{10.7} = 161$, and Ap = 50. A total of nine scans taken over a period of about 2 minutes were selected for the analysis. During this time the shuttle latitude changed from -50.9° to -54.3°, the longitude from 45.8° E to 56.6° E, and the altitude from 266.9 km to 268.1 km. The latitudinal and longitudinal dimensions of the atmosphere sampled were -35.9° to -54.3° and 15.3° E to 56.6° E. These geographic points in the southern hemisphere lie outside the auroral oval even for strong aurora (Whalen et al. 1985, Winick et al. 1985) and no portion of the line-of-sight, which traversed about 2.5° longitudinally for one degree change in latitude, was sunlit. The readings of the 391.4 nm and 557.7 nm photometers, corresponding respectively to the first negative band system (B→X) of N_2^+ and the $^1S \rightarrow {}^1D$ transition of atomic oxygen, the strengths of which are indicative of auroral activities, were inconclusive. However, comparisons between nighttime data taken in the auroral oval and those from the scans

used in our analysis show that at similar tangent heights the former have significantly larger band radiances. One comparison at a tangent height of about 200 km revealed that the auroral data has much enhanced signals in the hot as well as the thermal rotational components. We conclude that the atmosphere we sampled was not affected by auroral activity.

The data consist of radiometer limb radiances in the band pass 4.9 - 7.0 μm and high resolution limb spectra obtained by an unfiltered Michelson interferometer; the latter resolve the spin components of some of the rotational lines. The third harmonic of the ν_2 band of CO_2 near 2002 cm^{-1}, an artifact present in data collected at low tangent altitudes ($\leq$ 120 km), appears at frequencies far from the thermal component and does not influence its analysis. The data were processed using the least square fitting procedures described by Wintersteiner et al. (1990). The line positions and line strengths obtained from the molecular parameters of Amiot (1982) and ab initio dipole moment of de Vivie and Peyerimhoff (1988) were used to construct the spectra for the fitting procedure. Separate spectra for the $\Omega = 1/2$ and $\Omega = 3/2$ transitions were constructed. Figure 1a is a sample of the spectrum obtained at 148 km tangent altitude, 19.3 hr local time and latitude and longitude at the tangent point of -46.9° and 36.3°, respectively. Figure 1b is a fit of the spectrum, and Figure 1c is the difference between 1a and 1b. The fit has an effective temperature, averaged over the line-of-sight, of 625 K for the rotationally thermal component which consists of the 1→0 vibrational transition with a small contribution from the 2→1 transition. That the contribution of the 2→1 transition to the thermal component is indeed small can be inferred from the barely detectable R8.5 lines which are

located at the foot of the 1→0 Q branches near 1875 cm^{-1}. The contributions of the 3→2 and the higher vibrational transitions were found to be comparable to the instrumental noise. The ratio of the Ω=1/2 to Ω=3/2 spin state populations is a parameter in the fitting procedure. The inferred value of 1.9 for the ratio agrees with that obtained by Lipson et al. (1994), who carried out a similar analysis of CIRRIS-1A spectra. Figure 2a shows the data and Figure 2b repeats the fit shown in Figure 1b, but on a logarithmic scale. Clearly present in the data in the wings of the P and R branches is the emission from a rotationally hot component. Lines of the 1-0 and 2-1 vibrational transitions appear with an intensity of about 1 % of the rotationally thermal component. We discuss the rotationally hot component in section III.

Laboratory studies indicate that a thermal rotational population arises in the reaction

$$N(^2D) + O_2 \rightarrow NO(v,J) + O \qquad (3)$$

(Kennealy et al. 1978, Piper et al. 1987). However the steady-state population of $N(^2D)$ atoms at 148 km at 19.50 hr local time is of the order of 1000 cm^{-3} (Fesen and Roble 1994, Strickland et al. 1993) and the resulting rate of population of NO(v=1) is negligible compared to that by the impact excitation of NO(v=0). The observed spectrum (Fig. 1a) is almost entirely attributable to the 1→ 0 vibrational transition and is consistent with the absence of chemiluminescence due to reaction (3) and with the absence of significant auroral activity (Picard et al. 1987).

The calculated altitude profile of NO(v=1) depends on the rate coefficient k_1 of reaction (1). The rate coefficient for the quenching of NO(v=1) by oxygen atom impact,

the reverse of process (1), has been measured by Fernando and Smith (1979) to be $6.5\pm0.7\times10^{-11}$ cm^3s^{-1} at 296±3 K and by Glanzer and Troe (1975) to be $3.7\pm1.7\times10^{-11}$ cm^3s^{-1} at 2700 K. The value we chose was 6.0×10^{-11} cm^3s^{-1}, independent of temperature.

The SHARC Atmosphere Generator database (Adler-Golden 1995), based on the work of Smith et al. (1993), was used to obtain the NO density and the MSIS (Hedin 1987) model was used for the profiles of the densities of N, O, and O_2, and the temperature T. The $F_{10.7}$ index was 161.0 and the Ap index was 50. The latitude, longitude, and local time were chosen to correspond to the observed spectrum shown in Figure 1a. The atmosphere corresponding to this set of geophysical parameters we refer to as the "standard atmosphere." For the limited geographical space over which the data were taken, we use the plane parallel approximation for the standard atmosphere in which the densities and the temperatures are functions of altitude alone. The altitude profiles of the densities of N, O, O_2, and NO, and the temperature T for the standard atmosphere are illustrated in Figure 3.

Figure 4 compares the calculated altitude profile of the NO(v=1) population for the standard atmosphere with the profiles derived from the CIRRIS-1A measurements. The calculated profile is obtained by using reaction (1) as the production mechanism and emission at 5.3 μm as the loss mechanism. The CIRRIS(i) and CIRRIS(r) profiles were obtained, respectively, by inverting the radiances inferred from the fit to the interferometer data and those retrieved directly from the radiometer data using an algorithm of Sharma and Zachor (1985). The difference between the two experimental profiles is a measure of

their uncertainty. The agreement with the calculated profile is satisfactory given the uncertainties in the rate coefficient, the temperature, and the densities of O and NO(v=0).

Fig. 5a shows the spectrum calculated for the standard atmosphere, and Fig. 5b gives the difference between it and the observed spectrum from Fig. 1a. The difference is effectively eliminated by adopting a temperature at 148 km that is lower by 100 K than the MSIS temperature. This conclusion agrees with that reached by Sharma et al. (1996) who obtained local rotational temperatures of NO(v=1) in the terrestrial thermosphere by performing a temperature inversion of the interferometer data. The lower temperature reduces the excitation rate coefficient. To maintain the agreement in Figure 4, the product of the NO and O densities must be increased by a factor of about 1.5.

III. HIGHLY-EXCITED ROTATIONAL COMPONENT

The highly excited rotational component of the nitric oxide emission may be due to the chemical reaction (2). Theoretical studies have shown that the product molecule is both rotationally and vibrationally excited (Gilibert et al. 1993,1995, Duff et al. 1994). Energetic atoms may be a major source of vibrationally and rotationally excited NO during the daytime (Sharma et al. 1993), but at night the supply is limited (Sharma et al. 1995). However a major source of NO at night arises from the reactions of the thermal component of the velocity distribution of nitrogen atoms. To calculate the resulting emission spectrum, we adopted the calculations of Duff, Bien, and Paulsen (Private Communication 1995) for the vibrational and rotational distributions of the NO molecules resulting from process (2). Fig. 6 illustrates the corresponding production rates of the

nascent NO in the first five vibrational levels and the total rate for the standard atmosphere. The mean vibrational quantum number of the nascent NO is 4.2. The associated rotational distributions depend upon the altitude through the kinetic temperature T. They may be characterized by an effective rotational temperature T_r that increases from 2600 K at 130 km altitude where T= 572 K to 3350 K at 200 km altitude where T= 1025 K. The calculated rotational temperatures T_r are consistent with the value of about 3000 K obtained by Armstrong et al. (1994) from an average of eight nighttime scans varying in tangent heights between 139 and 141 km at local times between 19.40 and 19.87 hr.

IV. TWO-COMPONENT SPECTRA

Because reaction (2) has an activation energy of 0.3 eV (Baulch et al. 1973, Suzi Valli et al. 1995), only the small fraction lying on the high velocity tail of the thermal distribution of nitrogen atoms contributes to the formation of rotationally excited NO molecules and the resulting emission is much less intense than that arising from direct impact excitation by process (1). In Fig. 7, we present the calculated steady-state densities of the vibrationally excited NO molecules arising from the two mechanisms as functions of altitude for the standard atmosphere taking into account the effects of radiative cascading. Fig. 8 is a presentation of the radiances near 5.3 μm in the fundamental ($\Delta v=1$) vibrational bands. It shows that for a tangent altitude of 130 km, the intensity of emission from vibrationally excited rotationally nonthermal molecules by the chemical reaction (2) is 3.5% of the thermal emission and that it increases to 40% at a

tangent altitude of 200 km. The enhancement is due to the rapid increase of the rate coefficient of reaction (2) with temperature. The predicted ratio of 1.6% for rotationally nonthermal to rotationally thermal emission from the 1→0 vibrational transition at 140 km tangent altitude appears to be consistent with the observations of Armstrong et al. (1994).

Figure 9 compares the measured emission spectrum of Figure 2a with the spectrum obtained by combining the rotationally thermal emission from reaction (1) and the calculated rotationally hot emission from reaction (2). The rotationally thermal portion was taken to be the fit to the observed thermal spectrum given by Figure 1b. The rotationally hot component was obtained by using the line of sight radiance calculated in Figure 8 and a rotational temperature of 3000 K. The theoretical spectrum clearly shows the 1-0 bandhead at 2020 cm^{-1} and the 2-1 bandhead at 1990 cm^{-1}. The bandheads can also be discerned with some difficulty in the experimental spectra. The theoretical and experimental spectra are similar but the calculated extended P-branch radiance is about 2.5 times too intense. The discrepancy suggests that the degree of vibrational excitation in reaction (2) in the semi-classical calculations of Duff et al. is too large. The calculations of Gilibert et al. (1993, 1995) yield less vibrational excitation.

V. VARIABILITY OF NO EMISSION

With the establishment of process (1) as the major source of thermal emission and process (2) as the major source of rotationally enhanced emission from nitric oxide at night, we may explore the dependence of the emission spectrum on the geophysical conditions. We calculated the rates of production of NO(v=1) for two MSIS model

atmospheres in addition to the standard model, corresponding to -28.0° latitude, 102.6° longitude, F10.7 index = 161, Ap index = 34.0, day 119 of year 1991 and the atmospheres labeled evening and midnight corresponding to 7:12 PM and midnight, respectively. Figure 10 is a comparison of the rates of production of NO(v=1) for the three model atmospheres. The rates of production of NO in the three model atmospheres differ by factors of between two and three.

VI. COOLING DUE TO 5.3 μm EMISSION FROM NO

The 5.3 μm thermal emission from NO has long been recognized as an important cooling mechanism in the thermosphere (Kockarts 1980, Zachor et al. 1985). We plot the rates of cooling due to the rotationally hot chemiluminescent emission and the thermal emissions in Fig. 11 together with the cooling rate due to the 63 μm ($^3P_1 \rightarrow {}^3P_2$) transition of atomic oxygen, pointed out by Bates (1951) to be an important cooling mechanism in the thermosphere. We have assumed that the fine structure levels of atomic oxygen are in local thermodynamic equilibrium (Sharma et al. 1994). At high altitudes cooling due to chemiluminescent energy in chemically produced NO becomes comparable to that due to atomic oxygen, although both are smaller than cooling due to inelastic collisions of NO with O. At still higher altitudes cooling due to atomic oxygen becomes the dominant cooling mechanism (Bates 1951).

VII. CONCLUSIONS

The work presented here gives a quantitative analysis of the quiescent nonauroral nighttime 5.3 μm emission in the fundamental rotation-vibration band of nitric oxide. The rotationally thermal component of the emission consists primarily of the first fundamental ($v=1\rightarrow v=0$) band. Our analysis confirms that its upper state is populated by the collisions of atomic oxygen with the lower state. The rotationally hot component is created, as is its daytime counterpart, by the reaction of $N(^4S)$ atoms with O_2. While the daytime rotationally hot component is produced by the reaction of both the background $N(^4S)$ atoms and the nonthermal $N(^4S)$ atoms (Sharma et al. 1993) the reaction of the background $N(^4S)$ atoms constitute the only source at night, as suggested by Armstrong et al. (1994).

As indicated by earlier studies (Tohmatsu 1990) the rate of destruction of NO due to reaction with N atoms around 7:30 PM is larger than its rate of production and the NO density is decreasing. That the NO(v=1) densities as functions of altitude, obtained by inverting the radiometer and the interferometer data, are in good agreement with those obtained by our calculations (Fig. 4) lends support to our input standard atmosphere.

Cooling due to the chemiluminescent reaction at high altitudes is comparable to that due to the 63 μm emission from atomic oxygen, but much less than the cooling from collisionally excited NO.

ACKNOWLEDGMENTS

This research was in part supported by AFOSR under task 2303 EP and Phillips Laboratory project 007, in part by the National Science Foundation, Division of Atmospheric Sciences under Grant No. 93-20175, and in part by the National Aeronautics and Space Administration under Grant No. NAGW-1561. CIRRIS-1A was funded by BMDO under Program Management Agreement 1155, task 03-13 (natural backgrounds); special thanks are due Dr. W. Fredrick for generous support. The authors are grateful to Dr. J. Duff, Dr. F. Bien, and Dr. D. Paulsen for making the results of their trajectory calculations available to us before publication. Many helpful conversations with our colleagues Dr. P. Armstrong, Dr. W. Blumberg, Dr. J. Dodd, Dr. S. Miller, Dr. J. Wise, and Dr. J. Whalen are gratefully acknowledged. Dr. C. Fesen, Dr. R. Joseph, Dr. R. Roble, and Dr. D. Strickland kindly provided generous help through the use of their codes and databases. Special thanks are due Dr. S. Lipson who carefully read the manuscript and made constructive suggestions. A portion of the work was performed while RDS was at the Harvard-Smithsonian Institute for Theoretical Atomic and Molecular Physics and he would like to thank its staff for their hospitality.

FIGURE CAPTIONS

Figure 1. (a) NO fundamental vibration-rotation band emission spectrum near 1875 cm^{-1} observed by CIRRIS-1A. (b) The thermal spectrum corresponding to a rotational temperature of 625 K. (c) Difference Spectrum. The 2→1 R8.5 lines in (a) and (b) comprise the very weak feature located towards the blue of the strong 1→0 Q branch lines.

Figure 2. Data of Figure 1a and the fit of Figure 1b plotted on a logarithmic scale. The number in the parenthesis is the exponent.

Figure 3. $N(^4S)$, O_2, O, and NO densities and ambient temperature T for the standard atmosphere as functions of altitude.

Figure 4. Altitude profiles of NO(v=1) population derived from CIRRIS-1A measurements and calculated using the standard atmosphere.

Figure 5. (a) Fundamental vibration-rotation spectrum of NO calculated using the standard atmosphere. (b) Difference between the observed spectrum (Figure (1a)) and the calculated spectrum.

Figure 6. Rates of production of NO by the reaction of $N(^4S)$ atoms with O_2 in the first five vibrational levels, labeled v=0 - 4, as well as the total rate as functions of altitude for the standard atmosphere.

Figure 7. Steady-state densities of vibrationally excited NO molecules as a function of altitude. The vibrational levels are labeled by the quantum number v. The solid curves, labeled v=1 and v=2, are the densities arising from the collisional process (1).

Figure 8. Line-of-sight radiances from vibrationally excited NO molecules as a function of tangent altitude. The number in the parenthesis is the exponent.

Figure 9. (a) NO fundamental vibration-rotation band emission spectrum near 1875 cm^{-1} observed by CIRRIS-1A. (b) The spectrum obtained by adding the calculated rotationally hot component at 3000 K to the rotationally thermal component at a line-of-sight temperature of 625 K. The number in the parenthesis is the exponent. The feature in the calculated spectrum at 2020 cm^{-1} is the $1 \rightarrow 0$ bandhead and that at 1990 cm^{-1} is the $2 \rightarrow 1$ bandhead.

Figure 10. Altitude profiles of the rates of production of NO(v=1) by the two mechanisms for the standard model atmosphere (solid curve) and for two model atmospheres described in Sec. V. The dashed curve corresponds to the midnight atmosphere and the dash-dot curve to the evening atmosphere.

Figure 11. Rates of cooling ($eVs^{-1}cm^{-3}$) as functions of altitude for the standard model atmosphere for the chemiluminescent reaction 2 (solid line), for the inelastic collisions of NO with O (long dashed line), and fine structure transitions of atomic oxygen at 63 μm (short dashed line). The number in the parenthesis is the exponent.

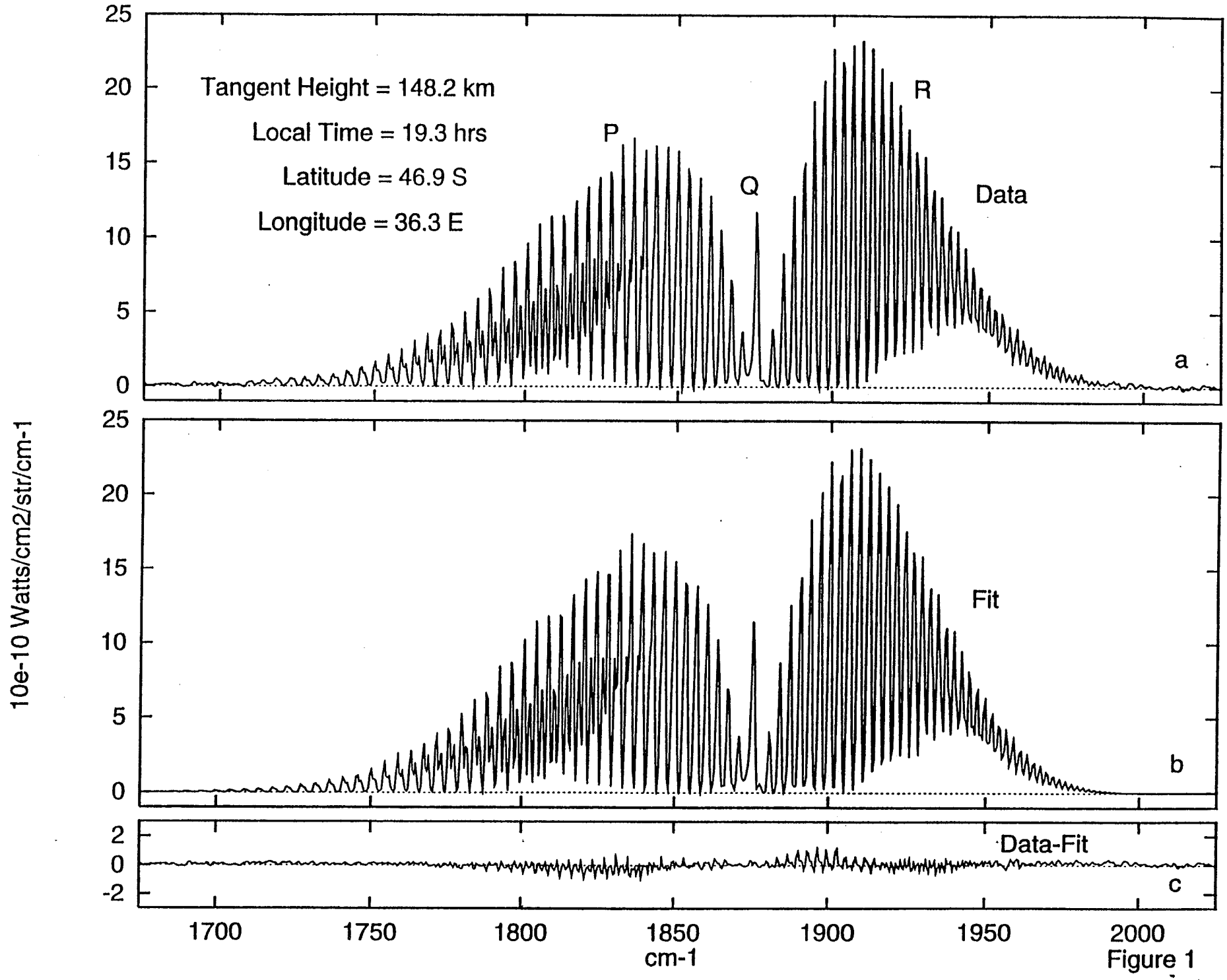
Tangent Height = 148.2 km
Local Time = 19.3 hrs
Latitude = 46.9 S
Longitude = 36.3 E
P
Q
R
Data
a
Fit
b
Data-Fit
c
10e-10 Watts/cm2/str/cm-1
cm-1
1700
1750
1800
1850
1900
1950
2000

Figure 1

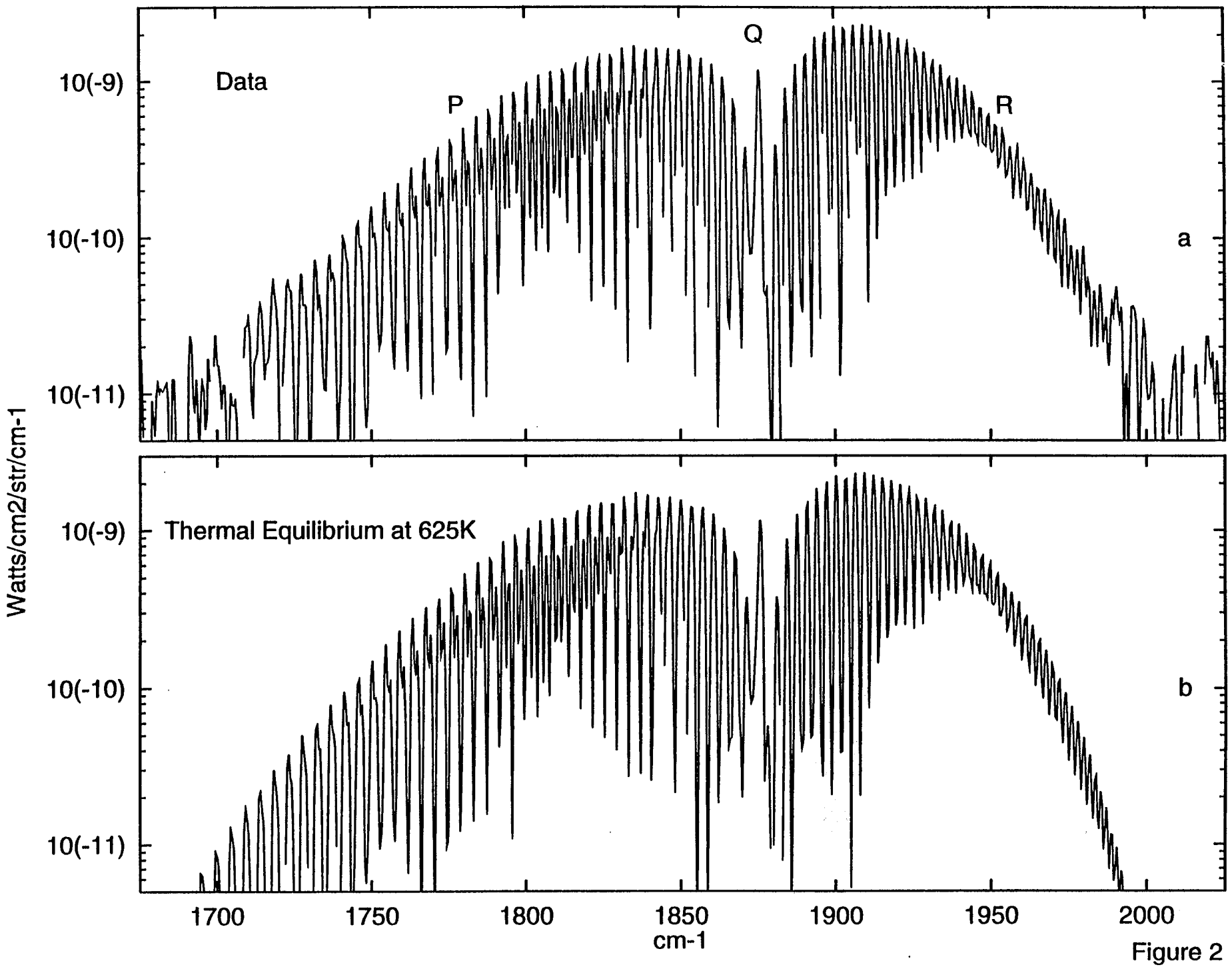
Data
P
Q
R
a
10(-9)
10(-10)
10(-11)
Thermal Equilibrium at 625K
b
Watts/cm2/str/cm-1
1700
1750
1800
1850
1900
1950
2000
cm-1

Figure 2

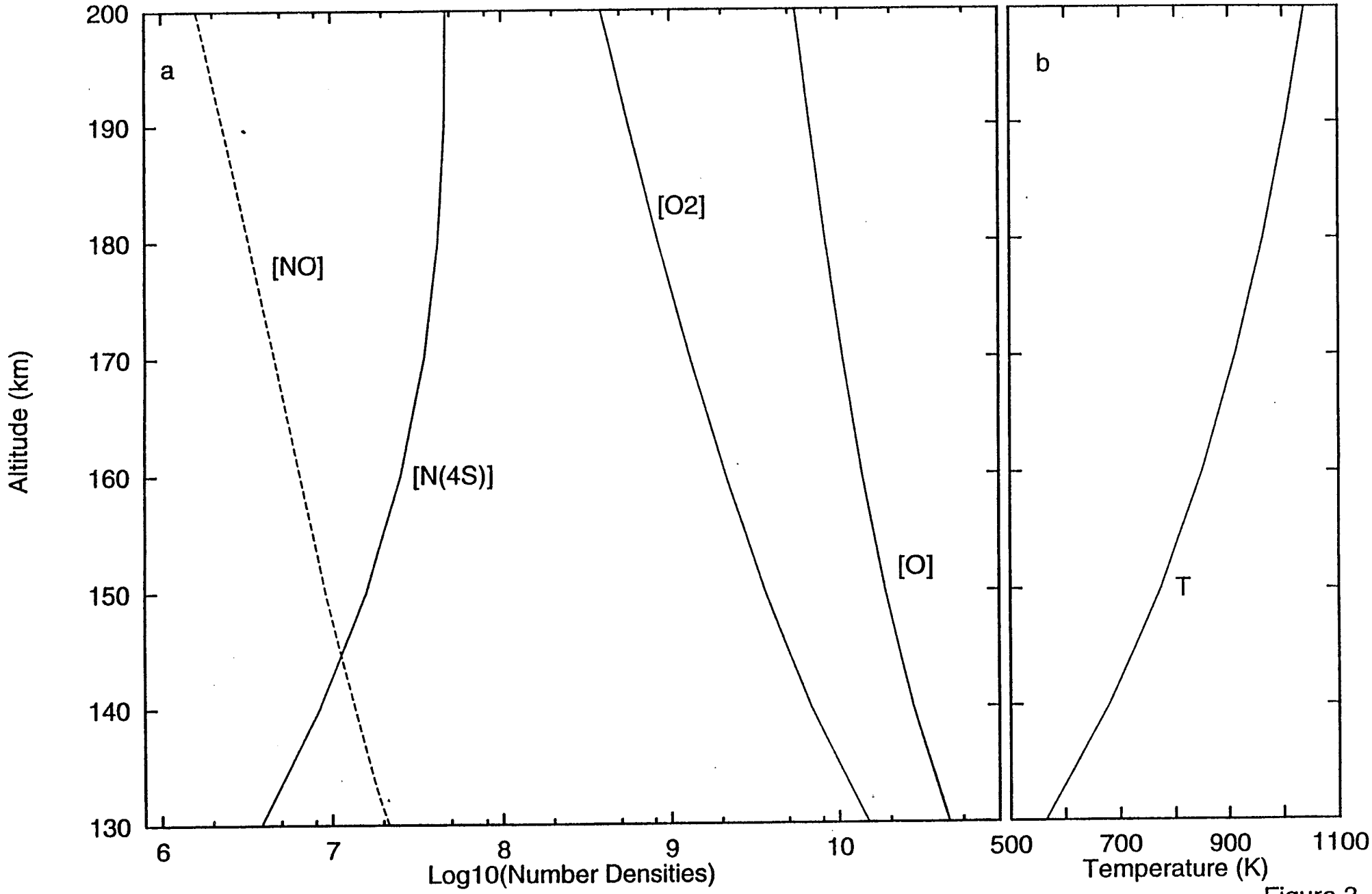
a
b
[NO]
[N(4S)]
[O2]
[O]
T
Altitude (km)
200
190
180
170
160
150
140
130
6
7
8
9
10
500
700
900
1100
Log10(Number Densities)
Temperature (K)

Figure 3

Fig. 4

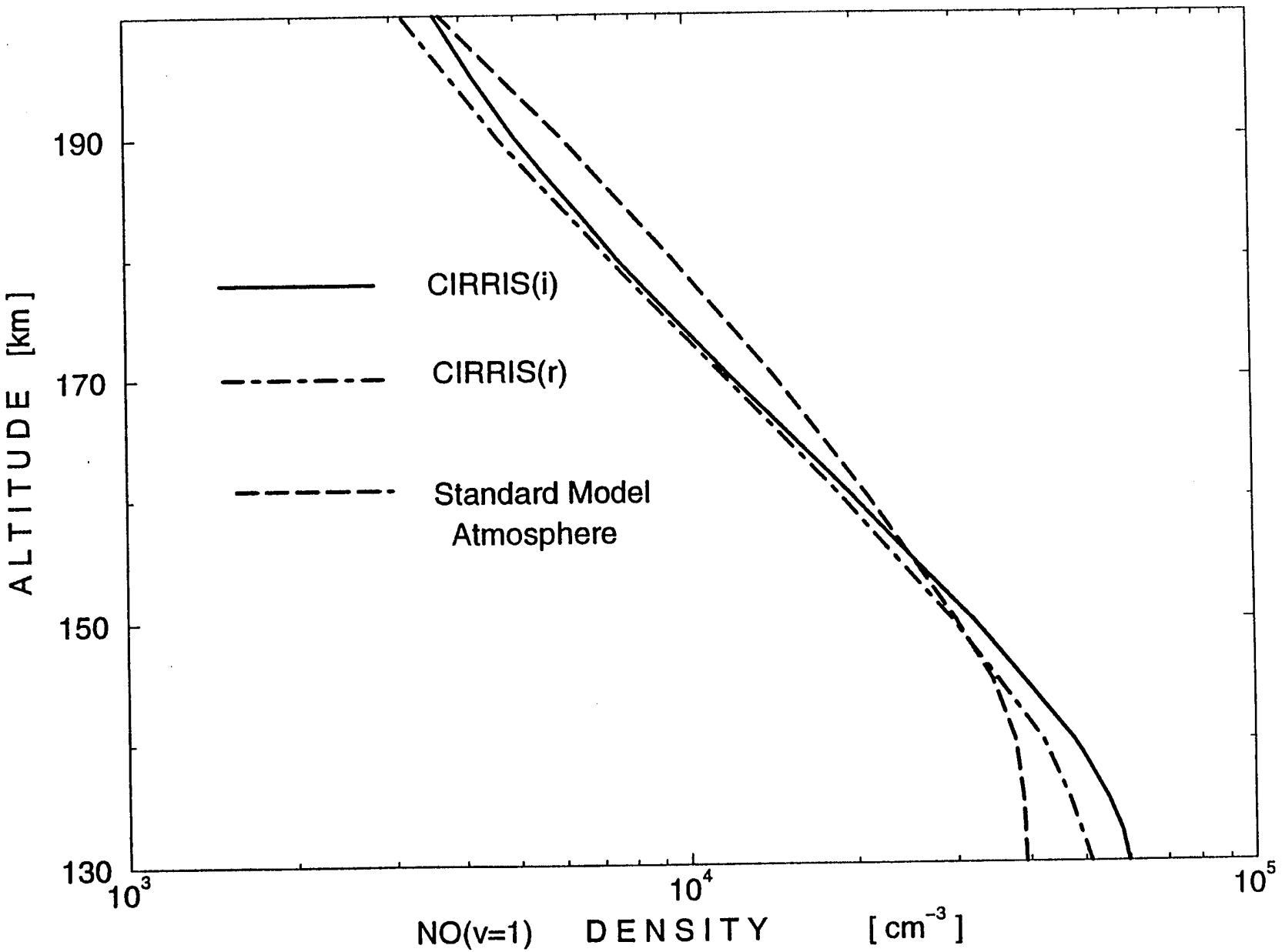
190
170
150
130
ALTITUDE [km]
CIRRIS(i)
CIRRIS(r)
Standard Model
Atmosphere
10^3
10^4
10^5
NO(v=1) DENSITY [cm^{-3}]

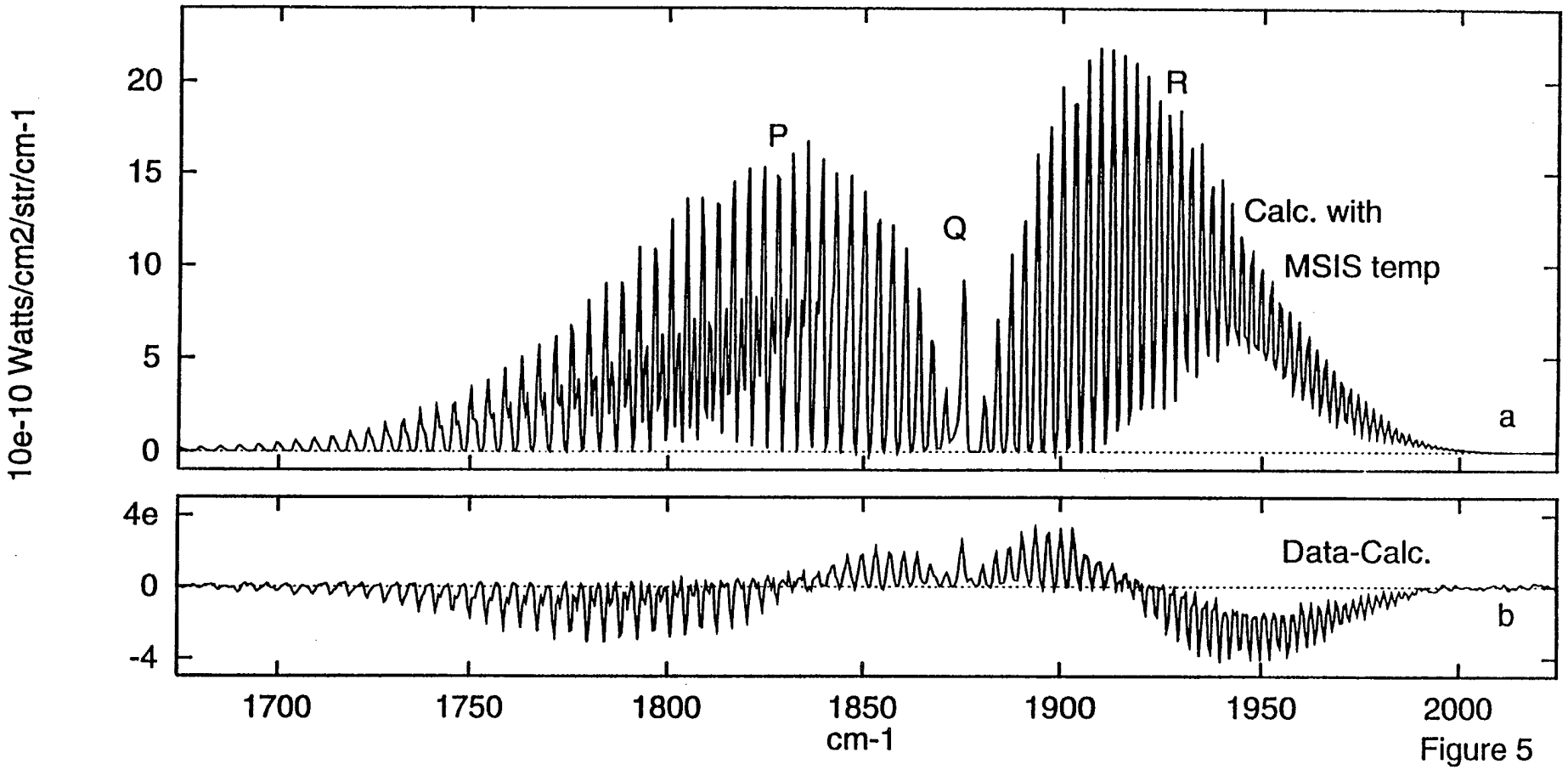
10e-10 Watts/cm2/str/cm-1
20
15
10
5
0
P
Q
R
Calc. with
MSIS temp
a
4e
0
-4
Data-Calc.
b
1700
1750
1800
1850
1900
1950
2000
cm-1

Figure 5

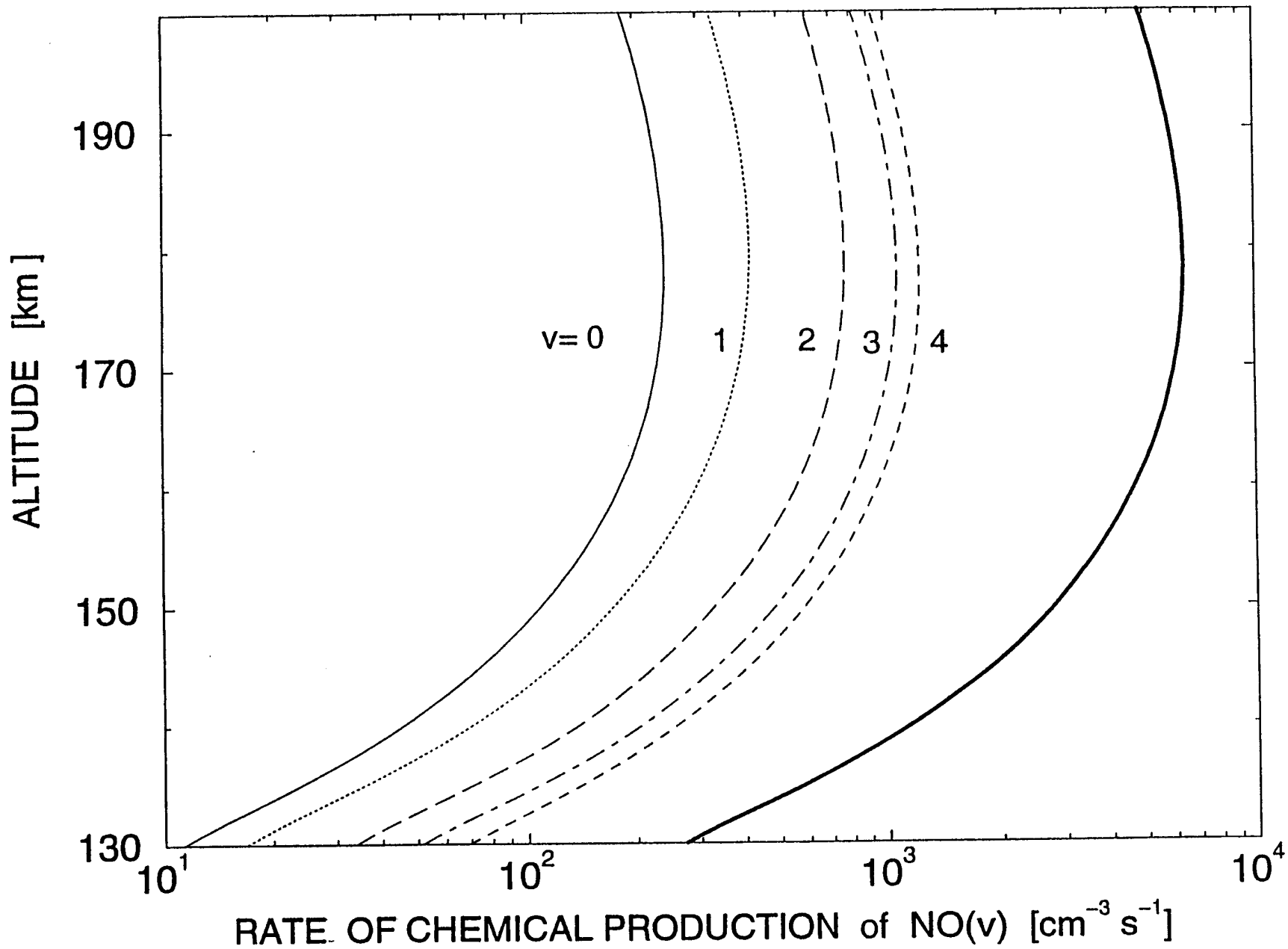
ALTITUDE [km]
190
170
150
130
v= 0
1
2
3
4
10^1
10^2
10^3
10^4
RATE OF CHEMICAL PRODUCTION of NO(v) [cm^{-3} s^{-1}]

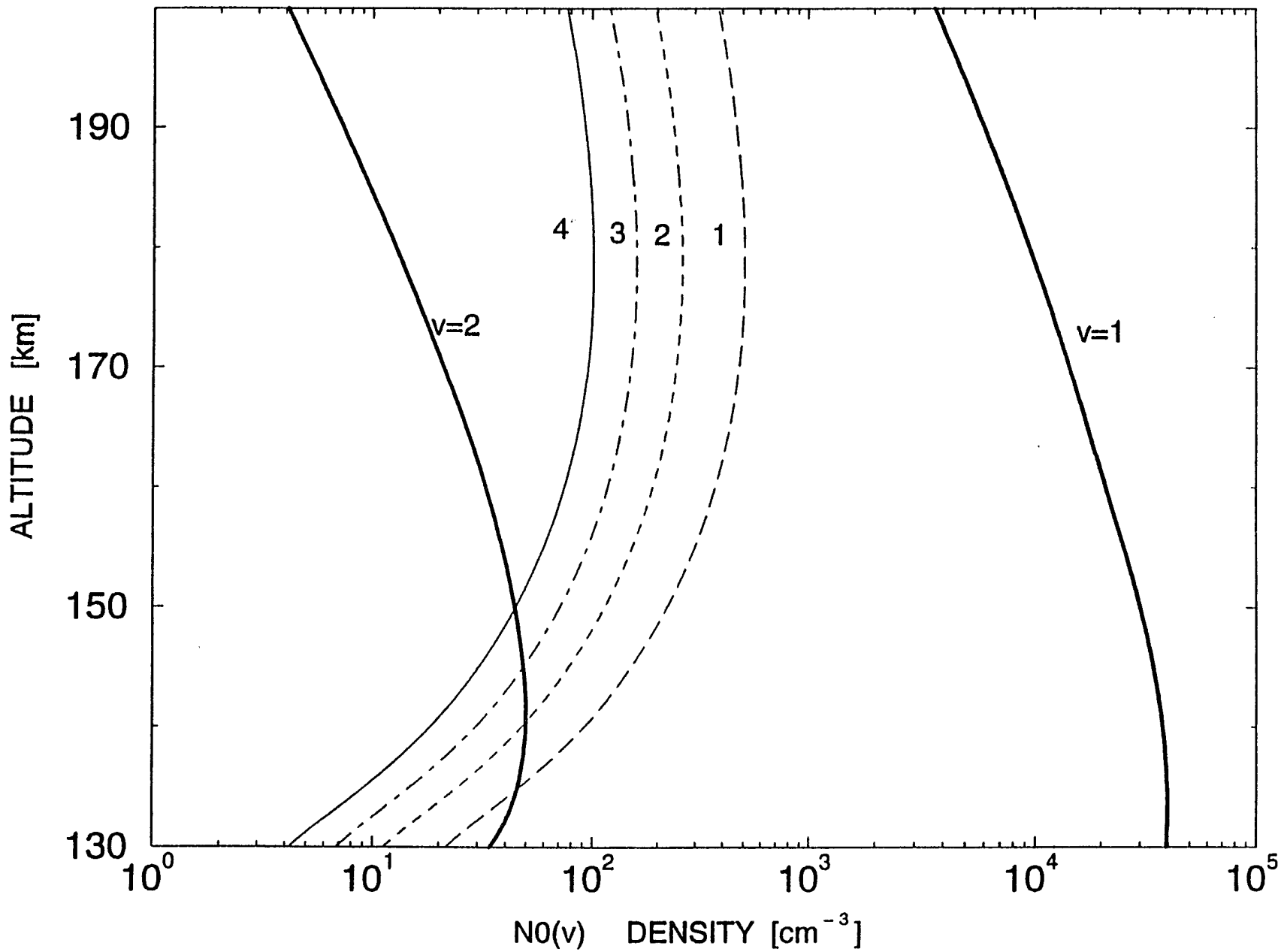
190
170
150
130
ALTITUDE [km]
v=2
4
3
2
1
v=1
10^0
10^1
10^2
10^3
10^4
10^5
N0(v) DENSITY [cm^{-3}]

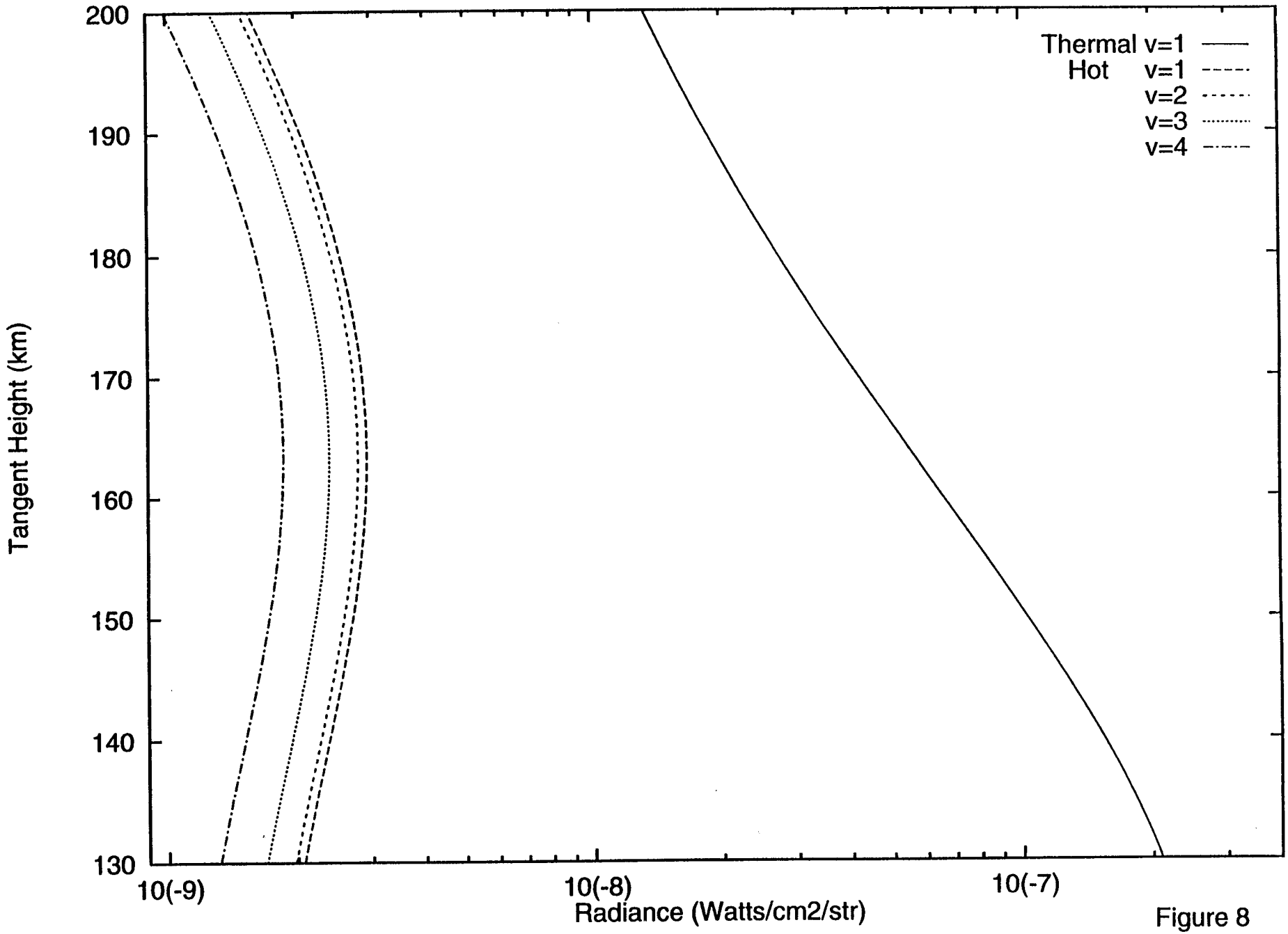
200
190
180
170
160
150
140
130
Tangent Height (km)
10(-9)
10(-8)
10(-7)
Radiance (Watts/cm2/str)
Thermal v=1
Hot v=1
v=2
v=3
v=4

Figure 8

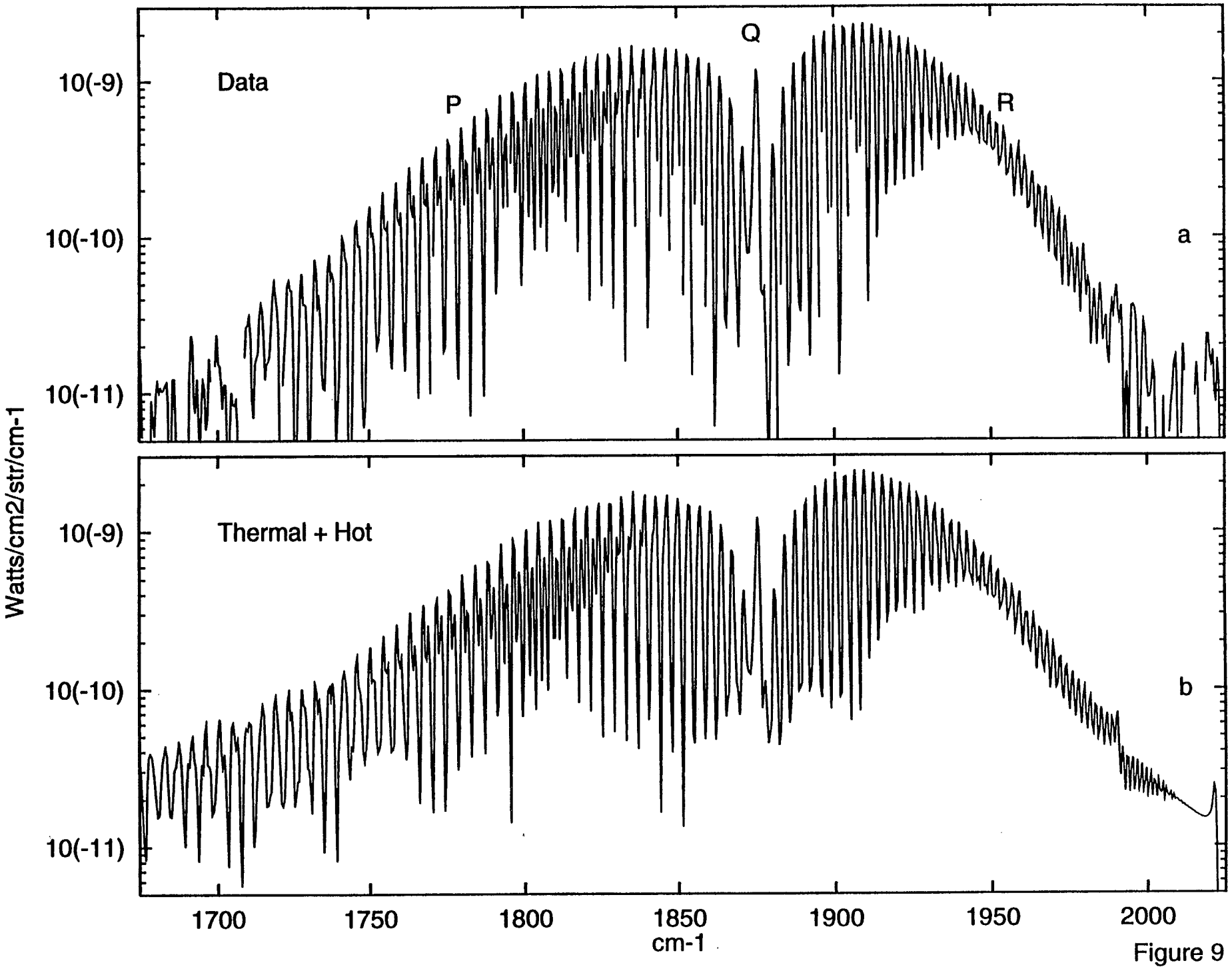
Data
P
Q
R
a
Thermal + Hot
b
10(-9)
10(-10)
10(-11)
Watts/cm2/str/cm-1
1700
1750
1800
1850
1900
1950
2000
cm-1

Figure 9

Fig 10

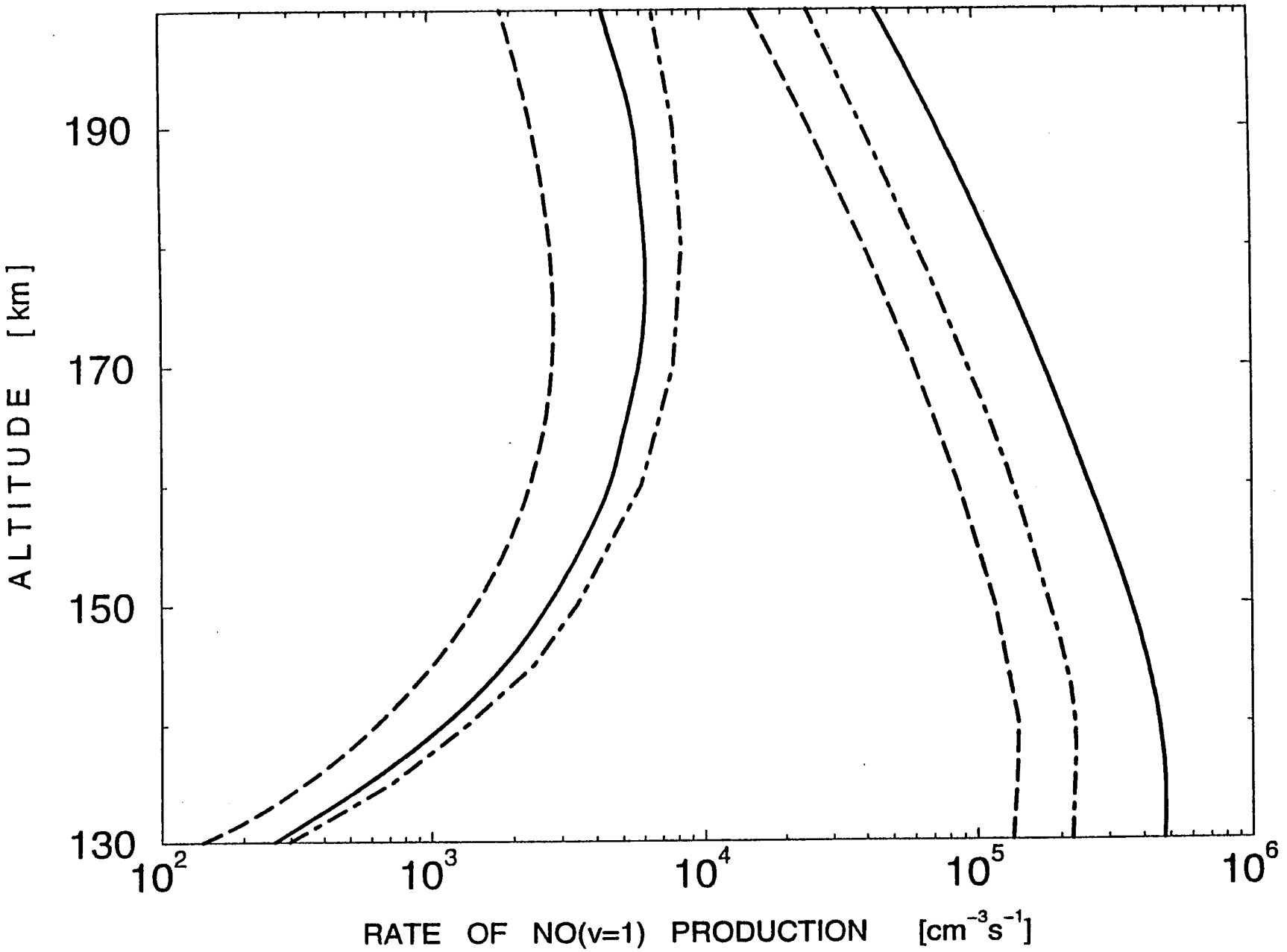
190
170
150
130
ALTITUDE [km]
10^2
10^3
10^4
10^5
10^6
RATE OF NO(v=1) PRODUCTION [$cm^{-3}s^{-1}$]

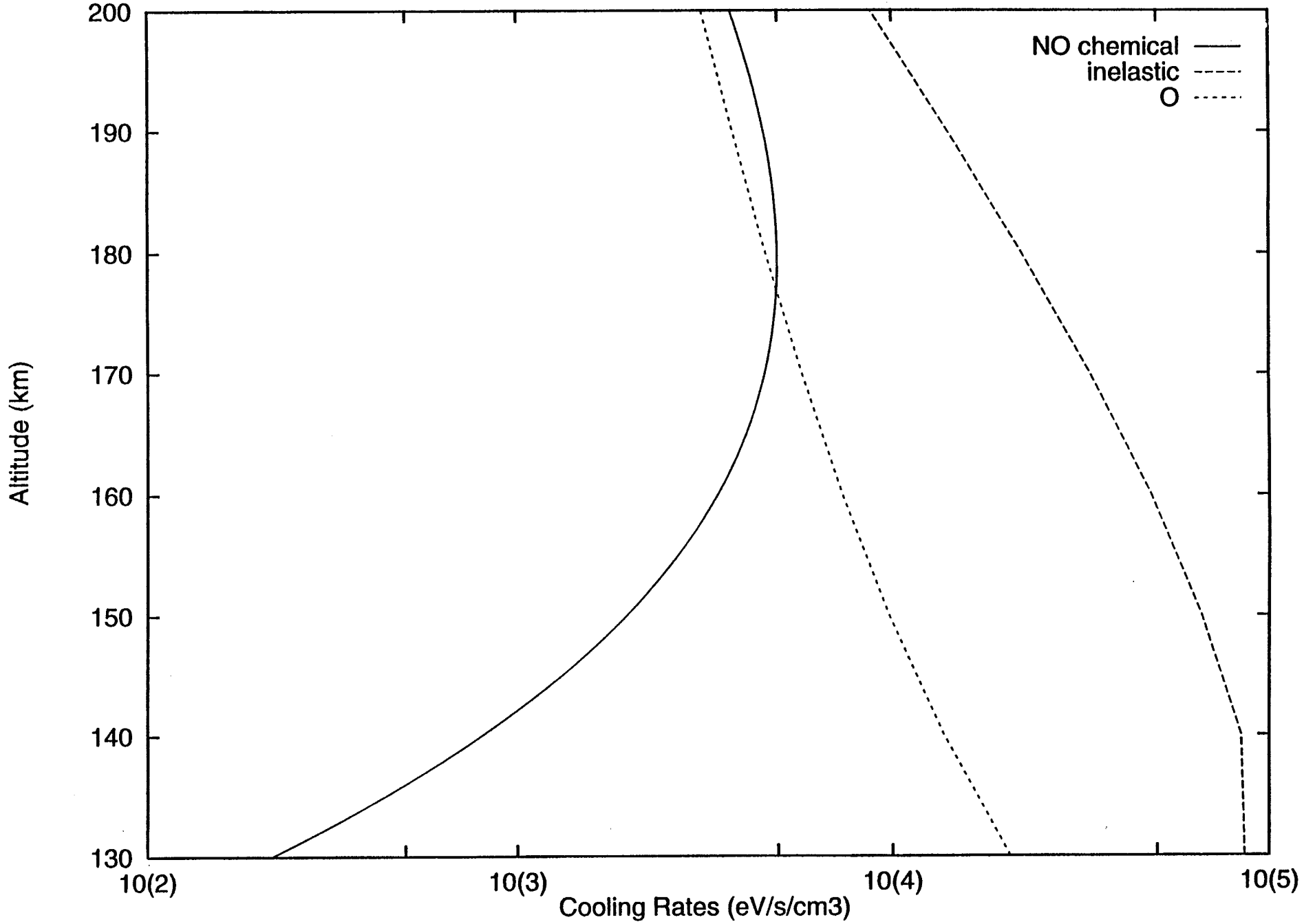
200
190
180
170
160
150
140
130
Altitude (km)
10(2)
10(3)
10(4)
10(5)
Cooling Rates (eV/s/cm3)
NO chemical
inelastic
O

Figure 11